LEARNING KOLMOGOROV MODELS FOR BINARY RANDOM VARIABLES

Anonymous authors
Paper under double-blind review

ABSTRACT

We propose a framework for learning a *Kolmogorov model*, for a collection of binary random variables. More specifically, we derive conditions that *link* (in the sense of implications in mathematical logic) outcomes of specific random variables and extract valuable relations from the data. We also propose an efficient algorithm for computing the model and show its *first-order optimality*, despite the combinatorial nature of the learning problem. We exemplify our general framework to recommendation systems and gene expression data. We believe that the work is a significant step toward interpretable machine learning.

1 INTRODUCTION

Machine learning and artificial intelligence method have permeated a large number of areas (Marr, Sept 2016). These methods are based on *machine learning models*, which consist of learning an input-output mapping for a given dataset. Despite the plethora of such models (e.g., matrix factorization (Koren et al., 2009), SVD-based models (Koren, 2008), deep neural networks (LeCun et al., 2015), and models inspired from physics (Stark, 2016b)), they lack *interpretability*: they are not capable of offering insight about the data, nor the underlying process. The lack of interpretablity may have serious consequences in mission-critical systems, ethics, and validation of computer-aided diagnosis (Doshi-Velez & Kim, 2017). While there is no consensus around the definition of interpretability, *causality* (Lipton, 2016) is a vital component: it refers to *causal relations* within the data and insight about the underlying data-generating process. We thus adopt a generalized version of causality using *implication* in mathematical logic as our 'definition' of *interpretable models*.

To this end, we propose learning a so-called *Kolmogorov Model (KM)* associated with a set of binary Random Variables (RVs). In addition to prediction, the interpretability of the model (as defined above) enables learning *causal relations*.[1] We derive a sufficient condition under which the realization of one RV's outcome (causally) *implies* the outcome of the other. In the context of recommendation systems, causal relations identify groups of items, for which a user liking one item *implies* that he/she likes all other items in the group. In gene expression analysis, the same relations identify groups of DNA locations for which the expression of a gene in one of them implies its expression in all other locations. The foundation of our approach is to model binary RVs as elementary events on a Kolmogorov space, by an inner product of two vectors (formally stated in Section 2.1), which is based on established results from classical probability theory. To our best knowledge, this specific formulation is novel in the context of learning representation.

The inner product of our formulation is reminiscent of factorization methods such as, matrix factorization (Koren, 2008), non-negative matrix factorization (Lee & Seung, 2001), SVD (Cai et al., 2010), and physics-inspired techniques, non-negative models (Stark, 2016a). It should be noted that the inner product components of these methods is usually based on strong intuition about the data, provided and validated by a human expert. In contrast, the proposed KM is a fully automated approach, deeply rooted in probability theory, which finds an interpretable model (as defined above) of the data without any human intervention. Thus, both the model and the causal relations within the data have a strong mathematical basis. Moreover, in most of the existing approaches, we may need to have one pipeline for learning the representation and another one for mining these relations. However, our approach requires only a single pipeline for both tasks. This is very appealing on a

[1] Hereafter, for the sake of simplicity, causal relations mean logical relations within the data.

conceptual level, and it can drastically simplify coding and validation. Our method also generalizes K-means and some of its variants. Detailed discussions of the relation between our proposed method and these prior works is in Appendix A.3.

In an abstract sense, we formulate a KM learning problem as a *coupled combinatorial program*, decompose it into two subproblems using the *Block-Coordinate Descent (BCD)* method, and obtain provably optimal solutions for both. For the first one, we exploit the structure of linear programs on the unit simplex and use low-complexity (yet optimal) *Frank-Wolfe* algorithm (Frank & Wolfe, 1956). To bypass the inherent complexity of the second subproblem (combinatorial and NP-hard), we propose a semidefinite relaxation, and show its *quasi-optimality* in recovering the optimal solution of the combinatorial subproblem. Finally, we show the convergence of our algorithm to a stationary point of the original problem. We propose a simple algorithm for mining the causal relations. All the proofs and additional discussions are available in Authors (Oct 2017).

2 System Model

Notation: Lowercase letter a, uppercase bold letter $\boldsymbol{A}$, and calligraphic letter $\mathcal{A}$ denote vectors, matrices, and sets, respectively. $[\boldsymbol{A}]_{i,j}$ and $\boldsymbol{A}^T$ denote element (i,j) and the transpose of $\boldsymbol{A}$. $\text{supp}(\boldsymbol{a})$ denotes the support set of $\boldsymbol{a}$. The inequality $\boldsymbol{x} \leq \boldsymbol{y}$ holds element-wise. $\boldsymbol{I}$ denotes the identity matrix, $\mathbf{1}$ and $\mathbf{0}$ the all-one and all-zero vectors (of appropriate dimension). $\boldsymbol{e}_n$ is the nth elementary basis, $\mathcal{P} = \{\boldsymbol{p} \in \mathbb{R}_+^D \mid \mathbf{1}^T\boldsymbol{p} = 1\}$ the unit simplex, and $\{n\} := \{1, \cdots, n\}$.

2.1 Problem Formulation

Consider a double-indexed set of binary *Random Variables (RVs)*, $X_{u,i} \in \mathcal{A} = \{1, 2\}$, taken from a dataset $\mathcal{D} = \{(u,i) \mid (u,i) \in \mathcal{U} \times \mathcal{I}\}$. Each RV is defined on a sample space Ω, consisting of *elementary events* $\Omega = \{\omega_d \mid 1 \leq d \leq D\}$. We denote by $\mathbb{P}[X_{u,i} = z],\ z \in \mathcal{A}$, the probability that RV $X_{u,i}$ takes the value $z \in \mathcal{A}$; see example in Section 2.2. Since $X_{u,i}$ is binary, it is fully characterized by considering one outcome. Thus, we write the *Kolmogorov Model (KM)* for $X_{u,i}$ as

$$\text{KM:} \qquad \mathbb{P}[X_{u,i} = 1] = \boldsymbol{\theta}_u^T \boldsymbol{\psi}_i \ . \tag{1}$$

Thus, each RV $X_{u,i}$ is associated with (characterized by) a *Probability Mass Function (PMF)* $\boldsymbol{\theta}_u, u \in \mathcal{U}$, and an *indicator vector* $\boldsymbol{\psi}_i, i \in \mathcal{I}$. The model follows from established results in classical probability theory (Gray, 2009) (formalized in Appendix A.2). Notice that the model in (1) can approximate with arbitrarily small accuracy the measure corresponding to $\mathbb{P}[\cdot]$ for a large enough D.

Problem 1 (Problem Statement) Let $p_{u,i}$ denote the *empirical value* of $\mathbb{P}[X_{u,i} = 1]$. We assume that $\{p_{u,i}\}$ are known for elements of a *training set* $\mathcal{K} \subseteq \mathcal{D}$, where $\mathcal{K} = \{(u,i) \mid (u,i) \in \mathcal{U} \times \mathcal{I}\}$.[2] Given samples coming from the model in (1), we wish to infer the parameters of underlying probability distribution: find parameters of the KM, i.e., $\{\boldsymbol{\psi}_i, \boldsymbol{\theta}_u\}$ that best describe $\{p_{u,i} \mid (u,i) \in \mathcal{K}\}$. The resulting problem is a *fully parametric statistical inference* task. For tractability, we address it using the minimum mean-squared error as a point estimator. The corresponding optimization problem is

$$(Q): \quad \{\boldsymbol{\psi}_i^\star, \boldsymbol{\theta}_u^\star\} \in \begin{cases} \underset{\{\boldsymbol{\psi}_i\},\{\boldsymbol{\theta}_u\}}{\text{argmin}} \sum\limits_{(u,i)\in\mathcal{K}} \left(\boldsymbol{\theta}_u^T\boldsymbol{\psi}_i - p_{u,i}\right)^2 \triangleq \mathcal{E} \\ \text{s. t. } \ \boldsymbol{\theta}_u \in \mathcal{P}\ ,\ \boldsymbol{\psi}_i \in \mathbb{B}^D,\ \forall (u,i) \in \mathcal{K} \end{cases} . \tag{2}$$

We present our solution to this *coupled non-convex conspiratorial* optimization in the next section. The obtained solution to (Q) can be used for prediction on a test set, as well as extracting causality structures within training set (see Section 4).

Proposed Approach: While the proposal to model binary RVs as elementary events on a Kolmogorov space is based on established results, the specific learning formulation (Problem 1) is novel. Because this model is rooted in probability theory, (1) defines the outcome of a RV in the *strict* Kolmogorov sense, and the resulting causal relations (Section 4) also hold from a strict analytical perspective. Note that causal relations (a.k.a. *association rules*) may still be extracted using existing methods, e.g., (non-negative) Matrix Factorization (MF) and their variants, SVD, binary MF, K-meas. However,

[2] The method for acquiring (estimates of) the empirical probabilities is application-dependent (see Section 5).

these relations are not based on causality and the formal relations that (mathematically) follow from the KM in (1), but rather on intuitions/heuristics, and yield different relations. Naturally, we wish the explore further in this work the causal relations that arise from the proposed model. Additionally, unlike existing methods, the prediction and causal relations mining are done in 'one-shot', thereby simplifying the implementation/validation; see Appendix A.3 for detailed discussions.

2.2 Illustrative Example: Recommendation Systems

In this context, $\mathcal{U}$ and $\mathcal{I}$ denote the set of users and items respectively, and $X_{u,i}$ models the preference of user u for item i, $(u,i) \in \mathcal{K}$. Thus, $\mathbb{P}[X_{u,i} = 1]$ (or $\mathbb{P}[X_{u,i} = 2]$) is the probability that user u likes (or dislikes) item i. Moreover, $\boldsymbol{\theta}_u$ determines the profile/taste of user u, $\boldsymbol{\psi}_i$ is related to item i (depending on genre, price, etc.), and the elementary events denote movie genres (e.g., $\omega_1 =$ "Action", $\omega_2 =$ "SciFi", etc.). The *training set*, consisting of an *empirical probability* that user u likes item i, $p_{u,i}$, is obtained as $p_{u,i} \triangleq [\boldsymbol{R}]_{u,i}/R_{\max}$, where $[\boldsymbol{R}]_{u,i} \in \mathbb{N}$ denotes the rating that user u has provided for item i, and $R_{\max}$ the maximum rating (Stark, 2015). For instance, if user u rates item i with a score of $[\boldsymbol{R}]_{u,i} = 7$ (where the maximum rating is 10), then t $p_{u,i} = .7$.

As a concrete illustrative example, consider a 10-star "recommendation system", having 2 users and 2 items. We then find the D-dimensional ($D = 3$) KM factorization to obtain , $\{\boldsymbol{\psi}_i^\star\}_{i=1}^2$ and $\{\boldsymbol{\theta}_u^\star\}_{u=1}^2$. D is the size of the Kolmogorov space Ω, the number of elementary events, and the dimension of the factorization (selected via cross-validation to minimize the test error). Solving (Q) results in finding $\{\boldsymbol{\psi}_i^\star\}_{i=1}^2$ and $\{\boldsymbol{\theta}_u^\star\}_{u=1}^2$. An example result is given below:

$$\underbrace{\begin{bmatrix} 0.3 & 1 \\ 0.1 & 1 \end{bmatrix}}_{\{p_{u,i}\}} = \begin{bmatrix} \boldsymbol{\theta}_1^{\star T} \{ & 0.2 & 0.3 & 0.5 \\ \boldsymbol{\theta}_2^{\star T} \{ & 0.1 & 0.1 & 0.8 \end{bmatrix} \begin{bmatrix} 0 & 1 & \}\text{Action} \\ 1 & 1 & \}\text{SciFi} \\ \underbrace{0}_{\boldsymbol{\psi}_1^\star} & \underbrace{1}_{\boldsymbol{\psi}_2^\star} & \}\text{Drama} \end{bmatrix}$$

To showcase the model's intuition, note that $p_{1,1}$, the probability that user 1 likes movie 1, is represented as $\boldsymbol{\psi}_1^T \boldsymbol{\theta}_1$. It is thus expressed as *convex/stochastic* mixture of *movie genres*, since elementary events are movie genres in this scenario. We underline that this high degree of interpretability is *not artificially* enforced but rather context-dependent. More generally, a KM represents a set of observed outcomes for RVs as (context-dependent) mixtures of elementary events. As the approach consists of learning a latent model, the performance and interpretability depends largely on D. Thus, the interpreting elements of the indicator vector as movie genres (as above) is one of the possible use cases of KMs. An in-depth investigation of these so-called highly interpretable models reveals that they perform rather poorly in terms of training/test error. This results points to a tradeoff between the level of interpretability and training/test performance (see Appendix A.4). We should reiterate that interpretability in this work is also done via the causal relations.

3 Proposed Algorithm

To approach a solution for problem (2), we use the *block-coordinate descent (BCD)* method to split (Q) into two sub-problems. Here, we derive our solution approach to each. We first refine the current PMF estimation $\boldsymbol{\theta}_u$, and then that of the indicator $\boldsymbol{\psi}_i$. Given $\{\boldsymbol{\psi}_i^{(n)}\}$ at iteration n, we pose the PMF refinement, θ-step, as

$$(Q_1) : \boldsymbol{\theta}_u^{(n+1)} \in \underset{\boldsymbol{\theta}_u \in \mathcal{P}}{\text{argmin}}\ f(\boldsymbol{\theta}_u) \triangleq \boldsymbol{\theta}_u^T \underbrace{\boldsymbol{Q}_u^{(n)}}_{:=\sum_{i\in\mathcal{I}_K} \boldsymbol{\psi}_i^{(n)} \boldsymbol{\psi}_i^{(n)T}} \boldsymbol{\theta}_u - 2\boldsymbol{\theta}_u^T \underbrace{\boldsymbol{r}_u^{(n)}}_{:=\sum_{i\in\mathcal{I}_K} \boldsymbol{\psi}_i^{(n)} p_{u,i}} . \quad (3)$$

We then pose the indicator vector refinement, ψ-step, as

$$(Q_2) : \boldsymbol{\psi}_i^{(n+1)} \in \underset{\boldsymbol{\psi}_i \in \mathbb{B}^D}{\text{argmin}}\ g(\boldsymbol{\psi}_i) \triangleq \boldsymbol{\psi}_i^T \underbrace{\boldsymbol{S}_i^{(n+1)}}_{:=\sum_{u\in\mathcal{U}_K} \boldsymbol{\theta}_u^{(n+1)} \boldsymbol{\theta}_u^{(n+1)T}} \boldsymbol{\psi}_i - 2\boldsymbol{\psi}_i^T \underbrace{\boldsymbol{v}_i^{(n+1)}}_{:=\sum_{u\in\mathcal{U}_K} \boldsymbol{\theta}_u^{(n+1)} p_{u,i}} . \quad (4)$$

Moreover, $\mathcal{U}_K$ and $\mathcal{I}_K$ are defined as $\mathcal{K} = \{(u,i) \mid u \in \mathcal{U}_K \subseteq \mathcal{U}\ ,\ i \in \mathcal{I}_K \subseteq \mathcal{I}\}$. Recall that having *globally optimal* solutions for both (Q_1) and (Q_2) is necessary to show the convergence of BCD (Tseng, 2001) - a challenging task due to the NP-hardness of (Q_2).

function $[\boldsymbol{\theta}_u^\star]$ = FW ($\boldsymbol{Q}_u, \boldsymbol{r}_u, \epsilon$)
  for $k = 1, 2, ..., I_{FW}$ **do**
    $\boldsymbol{d}_u^{(k)} = \boldsymbol{e}_{j^\star},\ j^\star = \underset{1\le j\le D}{\text{argmin}}\ [\nabla f(\boldsymbol{\theta}_u^{(k)})]_j$
    $\boldsymbol{\theta}_u^{(k+1)} = (1-\alpha_u^{(k)})\boldsymbol{\theta}_u^{(k)} + \alpha_u^{(k)}\boldsymbol{d}_u^{(k)}$
    Stop if $\|\boldsymbol{\theta}_u^{(k+1)} - \boldsymbol{\theta}_u^{(k)}\| \le \epsilon$
  end for
end function

Table 1: θ-step solution using FW

function $[\hat{\boldsymbol{\psi}}_i]$ = SDR ($\boldsymbol{S}_i, \boldsymbol{t}_i, M_{rnd}$)
  // Repeat to approximate each $\boldsymbol{\psi}_i^\star, \forall i \in \mathcal{I}_K$
  Solve (5) to find $\boldsymbol{X}_i^{(\text{SDR})}$
  Factorize as $\boldsymbol{X}_i^{(\text{SDR})} = \boldsymbol{L}_i^T\boldsymbol{L}_i$
  for $m = 1, 2, ..., M_{rnd}$ **do**
    Gen. zero-mean i.i.d Gaussian vector $\boldsymbol{u}_i^{(m)}$
    Compute $\hat{\boldsymbol{u}}_i^{(m)} = \text{sign}[\ \boldsymbol{L}_i^T\boldsymbol{u}_i^{(m)}\ ]$
  end for
  Find $m^\star = \text{argmin}_{1\le m\le D+1}\ \hat{\boldsymbol{u}}_i^{(m)^T}\tilde{\boldsymbol{S}}_i\hat{\boldsymbol{u}}_i^{(m)}$
  Compute $\hat{\boldsymbol{z}}_i = [\boldsymbol{u}_i^{(m^\star)}]_{1:D}\ [\boldsymbol{u}_i^{(m^\star)}]_{D+1}$
  Approximate $\boldsymbol{\psi}_i^\star$, as $\hat{\boldsymbol{\psi}}_i = (\hat{\boldsymbol{z}}_i + \mathbf{1})/2$
end function

Table 2: ψ-step solution using SDR

3.1 θ-STEP: REFINE PMF ESTIMATE

We use the *Frank-Wolfe (FW)* algorithm (Frank & Wolfe, 1956) to solve (Q_1) as a succession of Linear Programs (LPs) over the unit simplex. While LP solvers generally have similar complexity as quadratic program solvers, solving an LP reduces to searching for the minimum index - which is computationally efficient, when the LP is over the unit simplex. We summarized this FW variant for solving (Q_1); see also Jaggi (2013)[Algorithm 1]. Here, we drop the BCD iteration index, n, and just keep the FW iteration number, k, for notation simplicity. We first determine the *descent direction*: $\boldsymbol{d}_u^{(k)} \in \text{argmin}_{\boldsymbol{s}\in\mathcal{P}}\ \left(\nabla f(\boldsymbol{\theta}_u^{(k)})\right)^T\boldsymbol{s}$. The constraint $\boldsymbol{s}\in\mathcal{P}$ greatly simplifies the above LP and yields: $\boldsymbol{d}_u^{(k)} = \boldsymbol{e}_{j^\star},\ \ j^\star \in \text{argmin}_{1\le j\le D}\ [\nabla f(\boldsymbol{\theta}_u^{(k)})]_j$; see Proposition 2 (Appendix A.6). The solution follows from LPs over the unit probability simplex. Thus, finding the descent direction reduces to searching over the D-dimensional gradient vector (done in $\mathcal{O}(D)$). Then, the current value is updated using a simple step size rule, $\alpha_u^{(k)} = k/(k+1)$. Table 1 shows the θ-step solution, and Proposition 3 in Appendix A.6 characterizes its convergence.

3.2 ψ-STEP: REFINE INDICATOR ESTIMATE

To address the NP-hard nature of (Q_2), we propose a solution based on *Semi-Definite Relaxation and Randomization (SDR)*, and establish its *quasi-optimality*. We use the results of Ma et al. (2002)[Sec IV-C]) and a series of reformulations to rewrite (Q_2) in the following equivalent form (see Authors (Oct 2017) for all the derivations):

$$\boldsymbol{X}_i^\star \in \text{argmin}_{\boldsymbol{X}_i}\ \text{tr}(\tilde{\boldsymbol{S}}_i\boldsymbol{X}_i)\ \ ,\ \ \text{s. t.}\ \ \boldsymbol{X}_i \succeq \mathbf{0},\ [\boldsymbol{X}_i]_{k,k} = 1, \forall k\ ,\ \text{rank}(\boldsymbol{X}_i) = 1$$

where $\boldsymbol{X}_i = \boldsymbol{x}_i\boldsymbol{x}_i^T$, $\tilde{\boldsymbol{S}}_i = \begin{bmatrix}(1/4)\boldsymbol{S}_i & -\tilde{\boldsymbol{t}}_i/2\\ -\tilde{\boldsymbol{t}}_i^T/2 & 0\end{bmatrix}$, $\boldsymbol{x}_i = \begin{bmatrix}\boldsymbol{z}_i\\ w_i\end{bmatrix}$, $\boldsymbol{z}_i = 2\boldsymbol{\psi}_i - \mathbf{1}$, $w_i \in \{-1, +1\}$ is an auxiliary variable, and $\tilde{\boldsymbol{t}}_i \triangleq (\boldsymbol{v}_i - (1/2)\boldsymbol{S}_i\mathbf{1})$. The problem is then relaxed into a convex program,

$$\boldsymbol{X}_i^{(\text{SDR})} \in\ \text{argmin}_{\boldsymbol{X}_i}\ \text{tr}(\tilde{\boldsymbol{S}}_i\boldsymbol{X}_i)\ \ ,\ \ \text{s. t.}\ \ \boldsymbol{X}_i \succeq \mathbf{0},\ [\boldsymbol{X}_i]_{k,k} = 1, \forall k \tag{5}$$

$\boldsymbol{X}_i^{(\text{SDR})}$ may be solved using generic solvers. Then, a randomization procedure (Ma et al., 2002) extracts an approximate (binary) solution for (Q_2); see Table 2. This evidently raises the issue of the *sub-optimality gap* for SDR. Based on the results of Tan & Rasmussen (2001) and Luo et al. (2010), we show in Proposition 4 (see Appendix A.6) that SDR (Table 2) is optimal (asymptotically in D) in recovering the *binary solution* of (Q_2).

We highlight that the performance bound in Proposition 4 compares the quality of both the approximate *binary solution* offered by SDR (with respect to the optimal binary solution of (Q_2)), as well as their respective cost functions. The asymptotic optimality is empirically validated in Appendix A.7.

3.3 ALGORITHM DESCRIPTION

The BCD-based algorithm alternates between refining the indicator and PMF vectors; see Algorithm 1. Lemma 2 (Appendix A.6) shows its convergence to a stationary point of (Q).

Algorithm 1 Iterative computation of KMs

// Randomly Initialize $\{\boldsymbol{\theta}_u^{(1)} \in \mathcal{P}\}$
for $n = 1, 2, ...$ **do**
  Compute $\boldsymbol{S}_i^{(n)}$ and $\boldsymbol{t}_i^{(n)}$ using (4)
  Call $\hat{\boldsymbol{\psi}}_i^{(n)}$ = SDR($\boldsymbol{S}_i^{(n)}, \boldsymbol{t}_i^{(n)}, M_{rnd}$), $\forall i \in \mathcal{I}_K$
  Compute $\boldsymbol{Q}_u^{(n)}$ and $\boldsymbol{r}_u^{(n)}$ using (3)
  // Initialize FW with $\{\boldsymbol{\theta}_u^{(n-1)}\}$*, from previous iteration*
  Call $\boldsymbol{\theta}_u^{(n)^\star}$ = FW($\boldsymbol{Q}_u^{(n)}, \boldsymbol{r}_u^{(n)}, \epsilon$), for all $u \in \mathcal{U}_K$
end for

4 Interpretability via Causal Relation

4.1 Causal Relations

Once a solution is found using Algorithm 1, here, we propose a method to find causal relations among the RVs. More specifically, we compare the support set of each pair of RVs from the training set, $X_{u,i}$ and $X_{u,j}$, and check if there is any 'overlap' between their support set. Intuitively, this condition means that some of the elementary events (see Section 2.1) of one RV might be 'contained' in the elementary events of another. Consequently, the RVs are mutually related by causality, and the outcome of one determines that of the other. This insight is formalized here.

Proposition 1 (Inclusion of Support Set) *Consider two random variables $X_{u,i}$ and $X_{u,j}$ (belonging to the training set) whose KM are given by the model in* (1)*. If* $\text{supp}(\boldsymbol{\psi}_j) \subseteq \text{supp}(\boldsymbol{\psi}_i)$*, then the following two causal relations hold:*

$$X_{u,i} = 1 \text{ implies } X_{u,j} = 1 \text{ , and } X_{u,j} = 2 \text{ implies } X_{u,i} = 2 \text{ .} \tag{6}$$

Proof: See Authors (Oct 2017) for the proof.
Stated plainly, when the support set condition holds, the first outcome of $X_{u,i}$ implies the same outcome for $X_{u,j}$, and the second outcome for $X_{u,j}$ implies the second one for $X_{u,i}$, thereby implying a *mutual causal relation* among them (since $X_{u,i}$ influences $X_{u,j}$ and vice-versa). Note that our above definition of causality and causal relations is different than conventional ones in Pearl (2009)[Chap 2.8]. Moreover, our definition is distinct from Granger causality, due to the mutual coupling among the RVs in question.

We present next a special case of Proposition 1. When $\boldsymbol{\psi}_i = \mathbf{1}$, then $\text{supp}(\boldsymbol{\psi}_i) = \{D\}$, and $\text{supp}(\boldsymbol{\psi}_j) \subseteq \text{supp}(\boldsymbol{\psi}_i)$ holds, for any choice of $\boldsymbol{\psi}_j, \forall\, j \in \mathcal{I}_K$, where $\mathcal{I}_K$ defined in Section 3.

Corollary 1 (Maximally Supported RVs) *Let $\{\boldsymbol{\psi}_i,\ \boldsymbol{\theta}_u\}_{(u,i)\in\mathcal{K}}$ denote the KM associated with $\{\mathbb{P}[X_{u,i} = 1]\}_{(u,i)\in\mathcal{K}}$. We define $\mathcal{M}$ as set of RVs for which the support set of the indicator vector is one, i.e., $\mathcal{M} = \{i \mid \boldsymbol{\psi}_i = \mathbf{1}\}$. Then, the condition* $\text{supp}(\boldsymbol{\psi}_j) \subseteq \text{supp}(\boldsymbol{\psi}_i)$ *(Proposition 1) holds trivially $\forall\, j \in \mathcal{I}_K$. Thus, the causal relations in* (6) *hold, for every $i \in \mathcal{M}$.*

For maximally supported RVs, the realization of one outcome, $X_{u,i} = 1$, determines that of *all RVs of the set* $\{X_{u,j} = 1 \mid \forall j \in \mathcal{I}_K\}$.

Example 1 (Causal Relations in Recommendation Systems) In addition to prediction, recommendation systems are designed to accurately mine for *association rules*: if a user likes item i will he/she like another item j? Thus, the causal relations of Proposition 1 and Corollary 1 will be quite powerful, as we shall see. In the example of Section 2.2, note that $\text{supp}(\boldsymbol{\psi}_1) \subseteq \text{supp}(\boldsymbol{\psi}_2)$. Then, Proposition 1 yields: if user 1 (or user 2) likes movie 2 implies he/she also likes movie 1. Moreover, $X_{1,2}$ and $X_{2,2}$ are maximally supported RVs, since $\boldsymbol{\psi}_2 = \mathbf{1}$. Thus, Corollary 1 reads: If *any* user likes item 2, then this *causally implies* that he/she likes *all other items* in the training set.

Thus, our approach provides association rules that follow from *causal relations* between different RVs. Consequently, these relations are stricter (as they are rooted in Kolmogorov probability) than other methods for mining association rules, which are not based on causality.

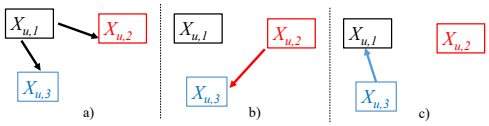

a) Check support set condition between $X_{u,1}$, and $X_{u,2}$, $X_{u,3}$ ($X_{u,1}$ is a maximally supported RV here)
b) Check support set condition between $X_{u,2}$, and $X_{u,1}$, $X_{u,3}$
c) Check support set condition between $X_{u,3}$, and $X_{u,1}$, $X_{u,2}$

Figure 1: Algorithm for CRM (toy example)

4.2 Causal Relations Mining (CRM)

We provide an efficient algorithmic approach to automatically mine the above relations. In a nutshell, the algorithm does a pairwise check of the support set condition (Proposition 1), for pairs of RVs $X_{u,i}$ and $X_{u,j}$, $\forall (i,j) \in \mathcal{I}_K \times \mathcal{I}_K$. The method is illustrated in Figure 1, for the illustrative example of Section 2.2.

The above causal relations can be modeled conveniently using the *adjacency matrix* $\boldsymbol{A} \in \mathbb{B}^{|\mathcal{I}_K| \times |\mathcal{I}_K|}$, defined as

$$[\boldsymbol{A}]_{i,j} = 1, \text{ if } \text{supp}(\psi_j) \subseteq \text{supp}(\psi_i), \text{ and } 0 \text{ otherwise}, \forall i \neq j \ . \tag{7}$$

Stated differently, $[\boldsymbol{A}]_{i,j} = 1$ if the support of $X_{u,j}$ is contained in that of $X_{u,i}$. Note that when $\boldsymbol{A}$ is sparse (resp. dense) is an indication for a dataset in which few (resp. many) casual relations exist. To quantify the sparsity level, we define an influence score, $\beta_i = |\mathcal{I}_K|^{-1} \sum_{\substack{j \in \mathcal{I}_K \\ j \neq i}} [\boldsymbol{A}]_{i,j}$, which measures the normalized number of pairs $X_{u,i}$ and $X_{u,j}$, satisfying the support set condition. These steps are summarized in the Algorithm 2 (illustrated in Figure 1). Moreover, its complexity is dominated by the pairwise search over $\mathcal{I}_K$ (see Step 1), which comes at $\mathcal{O}(|\mathcal{I}_K|^2 - |\mathcal{I}_K|) \approx \mathcal{O}(|\mathcal{I}_K|^2)$ operations.

Algorithm 2 Causal Relations Mining (CRM)

1. Check the support set condition, via a pairwise search to check for pairs $\boldsymbol{\psi}_i$ and $\boldsymbol{\psi}_j$ satisfying $\text{supp}(\psi_j) \subseteq \text{supp}(\psi_i)$, $\forall (i,j) \in \mathcal{I}_K \times \mathcal{I}_K$, $i \neq j$ (done over the training set $\mathcal{K}$)
2. Build the adjacency matrix $\boldsymbol{A}$, in (7) , and compute the influence score β_i, $\forall i \in \mathcal{I}_K$
3. Find all pairs (i,j) such that $a_{i,j} = 1$. For each of these pairs it holds that (Proposition 1), $X_{u,i}$ and $X_{u,j}$ are causally related, i.e.,

$$X_{u,i} = 1 \text{ implies } X_{u,j} = 1, \text{ and } X_{u,j} = 1 \text{ implies } X_{u,i} = 1 \tag{8}$$

4. Identify (if possible) maximally supported RVs (Corollary 1), $\mathcal{M} = \{i \mid \boldsymbol{\psi}_i = \mathbf{1}\}$. For each of them, the relations in (8) hold *for all* $i \in \mathcal{I}_K$

5 Special Cases and Applications

We highlight relevant special cases and applications of our approach.

Special Case: Unsupervised Learning Setting. Note that Algorithm 1 is equally applicable to an unsupervised learning task (no prediction needed). Moreover, if the training set has no missing data, i.e., $\mathcal{K} = \mathcal{D}$, then an alternate solution to (Q) may be obtained using the binary matrix factorization (MF) (Slawski et al., 2013) method. However, it *is not* applicable when factorizing a training set $\mathcal{K}$ (where $\mathcal{K} \subset \mathcal{D}$). Unlike Algorithm 1, binary MF does not offer prediction.

Application: Analysis of Gene Expression. The ability to analyze gene expression data is critical to DNA research (Zhang et al., 2009). This task can be formulated in our proposed framework as follows: $\mathbb{P}[X_{u,i} = 1]$ denotes the probability that the genes being studied are *expressed* in sample $u \in \mathcal{U}$ at location $i \in \mathcal{I}$ of the DNA. In this setting, the set Kolmogorov elementary events, $\{\omega_1, \cdots, \omega_D\}$, represents the *various genes* that might be involved. Consequently, our approach models the *probability that a set of genes is expressed as a convex mixture of D various genes*. We recall that this intuition follows from our model and is not enforced explicitly. More importantly, the causal relations can identify groups of DNA locations for which the expression of a gene (or its absence) in a given location implies its presence (or its absence) for all other locations in the group. We will numerically show the usefulness of these relations to DNA analysis, in Section 7.2.

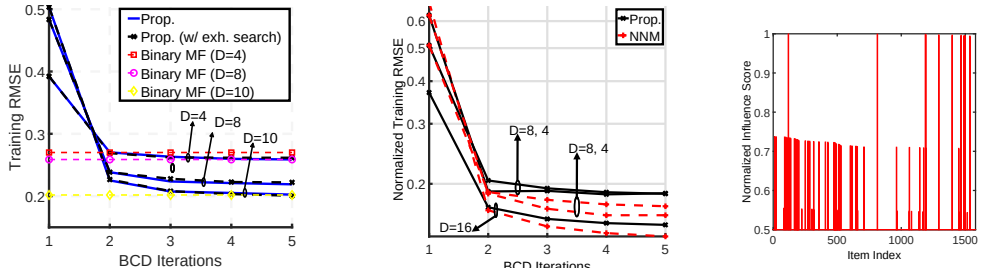

(a) Normalized Training RMSE vs Iterations (Setting 1)

(b) Normalized Training RMSE for KM vs NNM (Setting 2)

(c) Influence score β_i ($D = 8$, Setting 2)

Figure 2: Performance of proposed method

6 Practical Considerations

Overfitting: Regularization parameters (to mitigate overfitting) can be included without any changes to the solution method. An ℓ_2-regularization can be included in (Q_1): $f(\boldsymbol{\theta}_u) = \boldsymbol{\theta}_u^T(\boldsymbol{Q}_u + \lambda_u \boldsymbol{I}_D)\boldsymbol{\theta}_u - 2\boldsymbol{\theta}_u^T \boldsymbol{r}_u + \gamma_u$, where the regularizer $\lambda_u \geq 0$ is absorbed into a "new" matrix $(\boldsymbol{Q}_u + \lambda_u \boldsymbol{I}_D)$. Note that an ℓ_1-regularization for $\boldsymbol{\theta}_u$ would not work, since $\boldsymbol{\theta}_u \in \mathcal{P}$. Similarly, an ℓ_1-regularization for (Q_2) is: $g(\boldsymbol{\psi}_i) = \boldsymbol{\psi}_i^T \boldsymbol{S}_i \boldsymbol{\psi}_i - 2(\boldsymbol{v}_i - (\mu_i/2)\mathbf{1})^T \boldsymbol{\psi}_i + \gamma_i$, where the regularizer $\mu_i \geq 0$ is absorbed into the linear term, since $\mu_i \|\boldsymbol{\psi}_i\|_1 = \mu_i \mathbf{1}^T \boldsymbol{\psi}_i$, for $\boldsymbol{\psi}_i$ binary.
Optimality Gap: We recall that the proposed SDR method was shown to be quasi-optimal in providing approximate *binary solutions* to (Q_2). Thus, the relaxation does not affect the interpretability, in the sense that Proposition 1 and Corollary 1 still hold. While the derivations pertaining to causal relations (Section 4) assume globally optimal solutions to (Q) - an NP-hard problem, Algorithm 1 guarantees locally optimal ones. Thus, a bound on the gap between these solutions is needed. We highlight this issue as an interesting topic for further investigation.

6.1 Limitations

Computational Complexity: The computational complexity of Algorithm 1 is dominated by the solution in (5), which is $\approx \mathcal{O}(D^{4.5})$ operations per iteration of Algorithm 1 (recalling the negligible cost of the FW method). Notice that the additional complexity compared to matrix factorization (its extensions), for which the complexity is $\mathcal{O}(D^3)$, is not significant, especially that the size of the factorization in recommendations systems, D, is small. We also recall that D is relatively small ($D \leq 16$ in all numerical results). Moreover, we are are already investigating complexity reduction techniques leveraging the structure of the SDP, and distributed solutions to (P) to enable *parallelization*. Finally, the computational complexity of Algorithm 2 consists mainly of step 1, which has $\approx \mathcal{O}(|\mathcal{I}_K|^2)$ operations.

Learning a non-stationary distribution: The proposed method assumes that distributions of the RVs in the training set are stationary: Indeed, scenarios with *time-varying distributions* are a limitation (and interesting future directions). However, in learning it is quite common to assume that the data-generating distribution is stationary.

7 Numerical Results

7.1 Application to Recommendation Systems

Experimental Setup: We evaluate the performance of Algorithm 1 under the following. Hereafter, "Prop." refers to the proposed method.
Setting 1: An artificial training dataset, where $p_{u,i} \in \mathcal{K} = \{U = 20\} \times \{I = 40\}$, where $\{p_{u,i}\}$ are i.i.d. and uniformly chosen on the unit interval. We benchmark against a variant on Algorithm 1, where the ψ-step for Q_2 is replaced by an *exhaustive search*. As the data is artificial (unsupervised learning setting), we include the *Binary MF* in Slawski et al. (2013)[Algorithm 2].
Setting 2: The training set $\mathcal{K}$, is chosen as the MovieLens 100K, with $U = 943$ users and $I = 1682$

items, split into 80% for training and 20% for testing. Let $\{\hat{\boldsymbol{\psi}}_i\}, \{\hat{\boldsymbol{\theta}}_u\}$ the output of Algorithm 1, after 5 iterations. We benchmark against *matrix factorization (MF)* (Koren et al., 2009), *non-negative MF (NMF)* (Lee & Seung, 2001), *SVD++* (Koren, 2008) (ensuring the dimension of the factorization, k, is close to D), *non-negative models (NNM)* Stark (2015), and the K*-means (K-M)* algorithm. The implementation and results use the MyMediaLite package (Gantner et al., 2011).

Training Performance for Unsupervised Learning (Setting 1): Fig 2a shows the resulting normalized training RMSE $= (\sum_{(u,i)\in\mathcal{K}} |p_{u,i} - \hat{\boldsymbol{\theta}}_u^T \hat{\boldsymbol{\psi}}_i|^2/|\mathcal{K}|)^{1/2}$. We observe that the monotone convergence in Lemma 2 is validated numerically, and that the training error decays with increasing model size, D. Note that the training performance of Algorithm 1 is indistinguishable from its exhaustive search variant. Moreover, Algorithm 1 converges to solution whose performance is similar to Binary MF, with a few iterations (except for $D = 8$ where Algorithm 1 outperforms Binary MF).

Training Performance for Supervised Learning (Setting 2): Recall that Binary MF is not applicable here, due to the supervised learning setting. The same conclusions hold when testing Algorithm 1 on the ML100K (Figure 2b). We underline that while NNMs yield better training performance over Algorithm 1, the latter will have better test performance (since NNMs are indeed defined by relaxing KMs). In Table 4 (Appendix A.7), we empirically verify that the test performance of the proposed method outperforms the benchmarks in Setting 2.

Interpretability via Causal Relations (Setting 2): We numerically evaluate the relations of Algorithm 2. The influence score for each item in the training set, β_i, is shown in Figure 2c where we displayed items with *'high' influence score*, $\beta_i \geq 0.5$. Note that each of these high influence items is causally related to at *least half* of the items in the training set. This confirms the effectiveness of Algorithm 2 for finding causal relations, and that a sparse adjacency matrix is uncommon. We next identify the set of items corresponding to maximally supported RVs, $\mathcal{M} = \{119, 814, 1188, 1190, 1290, 1393, 1462, 1486, 1494, 1530, 1590, 1638\}$. For each of these items, a user liking one given item, implies he/she likes all other items in the training set. Interestingly, these results remain the same when $D = 24$, thereby suggesting that procedure for mining causal relations is quite stable.

7.2 Application to Gene Expression

Experimental Setup: Following the problem statement in Section 5, we show the usefulness Algorithm 2 for gene expression. We first define another setting.
Setting 3: We use the REGED0 dataset [3]. Element (u, i) in the input matrix, $[\boldsymbol{L}]_{u,i}$ represents the *level of gene expression* for sample u at location i of the DNA, and is reported as integer between 0 and $L_{\max}$. Similarly to recommendation systems (Section 2.2), the training set is obtained as $p_{u,i} := [\boldsymbol{L}]_{u,i}/L_{\max}$. Thus, $p_{u,i}$ denotes the (empirical) probability that the gene is expressed in sample u at location i. After running Algorithm 1, we use Algorithm 2 to mine causal relations. As this is unsupervised learning setting, we include the binary MF (Slawski et al., 2013) method.

Results: While Fig 3a shows the training performance for several values of D, Figure 3b plots the corresponding influence score that is obtained with our method. Fig 3a reveals a huge gap ($\approx 3\times$ less) between the training error of Algorithm 1 and Binary MF (unlike Figure 2a where both algorithms yield similar performance). This drastic degradation in the performance of binary MF compared to the small artificial of Figure 2a may be attributed to increasing the data/problem size (though we were unable to empirically verify this claim). Thus, we opted to use the solution of Algorithm 1 as a basis for finding causal relations. We identified 10 DNA locations corresponding to the highest β_i as: $\{813, 250, 774, 706, 380, 49, 477, 162, 740, 702\}$. For instance, the highest influence score of .1612 at DNA location 813 allowed to identify a set, $\mathcal{S}$, of 161 different locations which are *causally related* to DNA location 813. More specifically, the expression (or absence) of a given gene in location 813 implies its expression (or absence) in all other DNA locations in $\mathcal{S}$. While similar relations are possible using gene analysis methods, the above causal relations follow from our rigorous mathematical framework.

We also ran experiments on the ML 1M dataset (10x larger that ML 100K) and observed that main conclusions were the same. For lack of space, we instead opted to include different datasets such as the REGED0 dataset (5x larger than ML 100K) to exemplify another application of the approach.

[3] http://www.causality.inf.ethz.ch/data/REGED.html

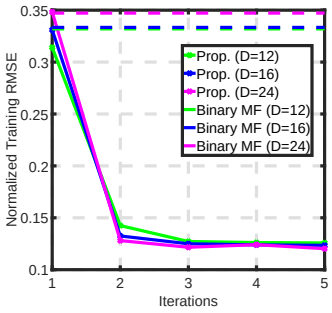

(a) Normalized Training RMSE as a function of iterations (Setting 3)

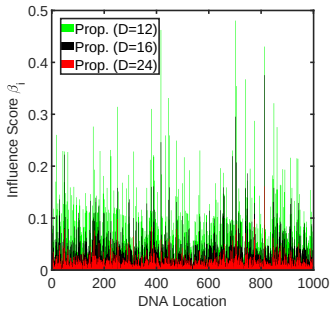

(b) Influence score for each DNA location (Setting 3)

Figure 3: Training performance of proposed method for REGED0 dataset

However, we note that a large-scale implementation of the method is not possible at this stage. As mentioned earlier, we are currently investigating complexity reduction methods before running experiments involving large datasets. Rather, the current work is intended a proof of concept of the usefulness of such an approach.

8 Conclusion

We have proposed a framework for learning a Kolmogorov model, associated with a collection of binary random variables. Interpretability of the model (as defined by logical implication and causality) was harnessed by deriving causal relations, i.e., by finding sufficient conditions that bind outcomes of certain random variables. We also proposed an algorithm for computing a Kolmogorov model, a combinatorial non-convex problem, and showed its convergence to a stationary point of the problem using results from block-coordinate descent. The combinatorial nature of the problem was addressed using a semi-definite relaxation. We also proposed an efficient algorithm to mine for the causal relations inherent to our model. Our results suggest that increased interpretability and improved prediction, do not cause a significant increase in complexity.

REFERENCES

Anonymous Authors. Learning elementary representations of random variables. *Technical Report*, Oct 2017. URL https://tinyurl.com/y7gpu4dc.

Jian-Feng Cai, Emmanuel J. Cands, and Zuowei Shen. A singular value thresholding algorithm for matrix completion. *SIAM Journal on Optimization*, 20(4):1956–1982, 2010. doi: 10.1137/080738970.

Mark Davenport and Justin Romberg. An overview of low-rank matrix recovery from incomplete observations. *IEEE Journal of Selected Topics in Signal Processing*, 10(4):608–622, June 2016. ISSN 1932-4553. doi: 10.1109/JSTSP.2016.2539100.

Finale Doshi-Velez and Been Kim. Towards a rigorous science of interpretable machine learning. *arXiv*, 2017.

Marguerite Frank and Philip Wolfe. An algorithm for quadratic programming. *Naval Research Logistics Quarterly*, 3(1-2):95–110, 1956. ISSN 1931-9193.

Zeno Gantner, Steffen Rendle, Christoph Freudenthaler, and Lars Schmidt-Thieme. Mymedialite: A free recommender system library. In *Proceedings of the Fifth ACM Conference on Recommender Systems*, RecSys '11, pp. 305–308. ACM, 2011. ISBN 978-1-4503-0683-6.

Robert M. Gray. *Probability, Random Processes, and Ergodic Properties*. Springer, 2nd edition, 2009. ISBN 1441910891, 9781441910899.

Patrik O. Hoyer. Non-negative matrix factorization with sparseness constraints. *CoRR*, cs.LG/0408058, 2004.

Martin Jaggi. Revisiting Frank-Wolfe: Projection-free sparse convex optimization. In *Proceedings of the 30th International Conference on Machine Learning*, volume 28, pp. 427–435, 2013.

Y. Koren, Robert Bell, and Chris Volinsky. Matrix factorization techniques for recommender systems. *Computer*, 42(8):30–37, Aug 2009. ISSN 0018-9162. doi: 10.1109/MC.2009.263.

Yehuda Koren. Factorization meets the neighborhood: A multifaceted collaborative filtering model. In *Proceedings of the 14th ACM International Conference on Knowledge Discovery and Data Mining*, KDD, pp. 426–434. ACM, 2008. ISBN 978-1-60558-193-4.

Yann LeCun, Yoshua Bengio, and Geoffrey Hinton. Deep learning. *Nature*, 521, 2015. doi: 10.1038/nature14539.

Daniel Lee and Sebastian Seung. Algorithms for non-negative matrix factorization. In *Advances in Neural Information Processing Systems (NIPS)*, pp. 556–562. MIT Press, 2001.

Zachary Chase Lipton. The mythos of model interpretability. *CoRR*, abs/1606.03490, 2016.

Stuart Lloyd. Least squares quantization in PCM. *IEEE Trans. Inf. Theor.*, 28(2):129–137, September 2006. ISSN 0018-9448. doi: 10.1109/TIT.1982.1056489.

Zhi-Quan Luo, Wing-Kin Ma, A.M.-C. So, Yinyu Ye, and Shuzhong Zhang. Semidefinite relaxation of quadratic optimization problems. *IEEE Signal Processing Magazine,*, 27(3):20–34, May 2010. ISSN 1053-5888. doi: 10.1109/MSP.2010.936019.

Wing-Kin Ma, T. N. Davidson, Kon Max Wong, Zhi-Quan Luo, and Pak-Chung Ching. Quasi-maximum-likelihood multiuser detection using semi-definite relaxation with application to synchronous CDMA. *IEEE Transactions on Signal Processing*, 50(4):912–922, April 2002.

Bill Marr. The top 10 AI and machine learning use cases everyone should know about. *Forbes Magazine*, Sept 2016.

Judea Pearl. *Causality: Models, Reasoning and Inference*. Cambridge University Press, New York, NY, USA, 2nd edition, 2009. ISBN 052189560X, 9780521895606.

Martin Slawski, Matthias Hein, and Pavlo Lutsik. Matrix factorization with binary components. In *Advances in Neural Information Processing Systems (NIPS)*, pp. 3210–3218, 2013.

Cyril J. Stark. Expressive recommender systems through normalized nonnegative models. *CoRR*, abs/1511.04775, 2015.

Cyril J. Stark. Expressive recommender systems through normalized nonnegative models. In *Proceedings of the Thirtieth AAAI Conference on Artificial Intelligence*, pp. 1081–1087, 2016a.

Cyril J. Stark. Recommender systems inspired by the structure of quantum theory. *CoRR*, abs/1601.06035, 2016b.

Peng Hui Tan and L. K. Rasmussen. The application of semidefinite programming for detection in CDMA. *IEEE Journal on Selected Areas in Communications*, 19(8):1442–1449, Aug 2001. ISSN 0733-8716. doi: 10.1109/49.942507.

P. Tseng. Convergence of a block coordinate descent method for nondifferentiable minimization. *Journal of Optimization Theory and Applications*, 109(3):475–494, 2001. ISSN 0022-3239. doi: 10.1023/A:1017501703105.

Joyce Jiyoung Whang, Inderjit S. Dhillon, and David F. Gleich. Non-exhaustive, overlapping k-means. In *Proceedings of the 2015 SIAM International Conference on Data Mining*, pp. 936–944, 2015. doi: 10.1137/1.9781611974010.105.

Zhong-Yuan Zhang, Tao Li, Chris Ding, Xian-Wen Ren, and Xiang-Sun Zhang. Binary matrix factorization for analyzing gene expression data. *Data Mining and Knowledge Discovery*, 20(1): 28, 2009. ISSN 1573-756X. doi: 10.1007/s10618-009-0145-2. URL `http://dx.doi.org/10.1007/s10618-009-0145-2`.

A SUPPLEMENTARY MATERIAL FOR LEARNING KOLMOGOROV MODELS FOR BINARY RANDOM VARIABLES

A.1 DEFINITIONS

A.2 KOLMOGOROV MODEL FOR A RANDOM VARIABLE

Let $(\Omega, \mathcal{M}, \mu)$ be a finite probability space. Here Ω is the sample space, the event class $\mathcal{M}$ is the power set of Ω, and μ assigns probabilities to the sets in $\mathcal{M}$. Let $X_{u,i}$ denote a doubly-indexed set of random variables on the given probability space, having output alphabet in $\mathcal{A}$, where elements of $\mathcal{A}$ are indexed by z, i.e., $\mathcal{A}(z)$ represents the zth element in $\mathcal{A}$. Also, let $\mathbb{P}[X_{u,i} = \mathcal{A}(z)] \in [0,\ 1]$ denote the probability that outcome $\mathcal{A}(z)$ occurs, for $1 \leq z \leq |\mathcal{A}|$. We let $\Omega = \{\omega_d \mid 1 \leq d \leq D\}$, where $\{\omega_d\}$ the set of all D-elementary events. Since $X_{u,i}$ is binary, i.e., $\mathcal{A} = \{1, 2\}$, we write the KM for $X_{u,i}$ as,

$$\begin{aligned} \mathbb{P}[X_{u,i} = 1] &= \boldsymbol{\theta}_u^T \boldsymbol{\psi}_{i,1} \\ \mathbb{P}[X_{u,i} = 2] &= \boldsymbol{\theta}_u^T \boldsymbol{\psi}_{i,2} = 1 - \boldsymbol{\theta}_u^T \boldsymbol{\psi}_{i,1}, \end{aligned} \tag{A.1}$$

where $\boldsymbol{\theta}_u$ is a *Probability Mass Function (PMF)* vector on the unit simplex, $\mathcal{P}$, and $\{\boldsymbol{\psi}_{i,1}, \boldsymbol{\psi}_{i,2}\} \in \mathbb{B}^D$ are *binary indicator vectors* representing the support of its probability measure. Moreover, the last equality follows from $\boldsymbol{\psi}_{i,1} + \boldsymbol{\psi}_{i,2} = \mathbf{1}$, which in turn follows from the outcomes of each RV summing to one. Since $X_{u,i}$ is binary, it is fully characterized by considering one outcome,

$$\mathbb{P}[X_{u,i} = 1] = \boldsymbol{\theta}_u^T \boldsymbol{\psi}_i, \tag{A.2}$$

A.3 RELATED WORK

Matrix Factorization Methods: Note that, (Q) can be re-written as a low-rank matrix factorization problem, over the set of binary and stochastic matrices (see Appendix A.5. Thus, the proposed approach is connected to factorization methods: *Matrix Factorization (MF)* (Koren et al., 2009), *Nonnegative Matrix Factorization* (Lee & Seung, 2001), SVD (Cai et al., 2010) (and their many variants/extensions) have gained widespread applicability, covering areas in sound processing, (medical) image reconstruction, recommendation systems and prediction problems (Davenport & Romberg, 2016). These techniques model elements of the training set as inner product of two *arbitrary vectors*: Despite their success, the performance is inherently *tied to the validity of that model*, and consequently the extent to which these assumption hold. However, this inner product does not represent a RV (in a mathematical sense), when viewed in the context of the proposed model (see Section 2.1). Consequently, the analytical guarantees of Section 4, which underpin the causal relations, do not hold for general factorization methods.

Nonnegative Sparse MF: It was empirically shown that the two low-rank components that are offered by sparse nonnegative MF (another variant of MF) provide insight (relations) on the data they model (see the numerical examples of Hoyer (2004)). While our proposed method also provides insight among the data (via the causal relations), the proposed KM and causal relations that are derived from it, are based on established axioms in probability. Unlike the relations offered by nonnegative sparse MF which are shown empirically, the causal relation in Section 4 hold analytically.

Binary MF: We underline that most MF methods also rely on BCD methods (alternating minimization), for which globally optimal solutions to each subproblem are needed for convergence. Thus, these methods cannot be *directly* applied to (Q), due to the binary constraints on $\boldsymbol{\psi}_i$. The authors are unaware generic solution approaches for (Q). Nonetheless, the *Binary MF* method (Slawski et al., 2013) can solve (Q) when the problem is *feasible* and the training set spans the *entire* data set, i.e., $\mathcal{K} = \mathcal{D}$. However, the method operates in the *unsupervised learning* setting only, without providing prediction (see Section 5). This indeed limits the applicability of binary MF to practical scenarios, since real-world data will have missing/erroneous data.

Clustering Methods: Consider a special case of (Q), where $\boldsymbol{\psi}_i$ is constrained to have one non-zero element. The resulting problem becomes the well-known *K-means clustering* (Lloyd, 2006). The K-means algorithms (and its variants K-medoids, fuzzy K-means and K-SVD), have become pervasive in an abundance of applications such as clustering, classification, image segmentation,

DNA analysis, online dictionary learning, source coding, etc. Our approach *generalizes K-means*, by allowing for overlapping clusters. While a similar generalization of the classical K-means algorithm was considered in (Whang et al., 2015), the number of points per cluster is determined explicitly.

Nonnegative Models: *Non-Negative Models (NNMs)* (Stark, 2016a) are recent attempts at interpretable models. For reasons of computational tractability (Stark, 2016a), NNMs are defined by relaxing $\boldsymbol{\psi}_i$ in (1). However, this relaxation *impairs* the highly interpretable nature of the model in (1), making causal relations *less accurate*.

A.4 Highly Interpretable Models

Consider the case where the elementary events correspond to each of the movie genres, i.e., $\Omega = \{\omega_1, \cdots, \omega_D\} = \{$"Action", $\cdots$, "SciFi"$\}$. We refer to this as *highly Interpretable Models*, due to their extremely interpretable nature: $\mathbb{P}[X_{u,i} = 1] = \boldsymbol{\psi}_i^T \boldsymbol{\theta}_u = \boldsymbol{t}_i^T \boldsymbol{\theta}_u$ is expressed as a convex/stochastic mixture of movie genres. These models are a 'holy grail' for recommendation systems. In this case, $\boldsymbol{t}_i$ is a binary genre tag vector with $[\boldsymbol{t}_i]_m = 1, \forall\, m \in \{D\}$, if movie i belongs to movie genre m, and zero otherwise. Now consider a genie-aided setting, where the set of movie genre tags $\{\boldsymbol{t}_i\}$, are known (and consequently $\{\boldsymbol{\psi}_i\}$ are known as well). Then, one can revisit the optimization problem for determining the KM, (P), where the indicator vectors are given, $\{\boldsymbol{\psi}_i = \boldsymbol{t}_i\}$, and the optimization is performed over the pmf vectors only $\{\boldsymbol{\theta}_u\}$:

$$\min_{\boldsymbol{\theta}_u \in \mathcal{P}} \boldsymbol{\theta}_u^T \Big(\sum_{i \in \mathcal{I}_K} \boldsymbol{t}_i \boldsymbol{t}_i^T \Big) \boldsymbol{\theta}_u - 2 \boldsymbol{\theta}_u^T \Big(\sum_{i \in \mathcal{I}_K} \boldsymbol{t}_i p_{u,i} \Big) + \gamma_u \tag{A.3}$$

However, numerical result reveal that the training and test performance of these representations is quite poor. We tested the performance of this highly interpretable model, by extracting the tag vectors $\{\boldsymbol{t}_i\}$ from the ML 100K dataset, and using them to optimize the corresponding pmf vectors. We set $D = 19$ to match the total number of movie genres for the ML 100K dataset. As seen in Table 3,

Training RMSE	Test RMSE
0.4468	0.4468

Table 3: Normalized errors metrics for highly interpretable models (ML100K).

the highly interpretable models have poor performance. This suggests the existence of a trade-off between the expressiveness and prediction performance.

A.5 Problem Formulation in Matrix Form

Let $\boldsymbol{\Psi} = [\boldsymbol{\psi}_1, \cdots, \boldsymbol{\psi}_I]$, $\boldsymbol{\Psi} \in \mathbb{B}^{D \times I}$ denote the aggregate indicator matrix (containing all the individual indicator vectors), $\boldsymbol{\Theta} = [\boldsymbol{\theta}_1, \cdots, \boldsymbol{\theta}_U]$, $\boldsymbol{\Theta} \in \mathbb{R}_+^{D \times U}$ the aggregate matrix of PMF vectors, and $[\boldsymbol{P}]_{(u,i)} = p_{(u,i)}, \forall (u,i) \in \mathcal{U} \times \mathcal{I}$, $\boldsymbol{P} \in \mathbb{R}_+^{U \times I}$ the aggregate matrix of known probabilities. Then, (Q) can be written in equivalent matrix form,

$$\begin{cases} \min\limits_{\boldsymbol{\Psi}, \boldsymbol{\Theta}} \ \mathcal{E}(\boldsymbol{\Psi}, \boldsymbol{\Theta}) = \| \boldsymbol{M} \circ \big(\boldsymbol{\Theta}^T \boldsymbol{\Psi} - \boldsymbol{P} \big) \|_F^2 \\ \text{s. t.} \quad \boldsymbol{\Psi} \in \mathbb{B}^{D \times I}, \ \boldsymbol{\Theta} \in \mathbb{R}_+^{D \times U}, \ \boldsymbol{\Theta}^T \mathbf{1} = \mathbf{1} \ . \end{cases} \tag{A.4}$$

where $\circ$ denotes the Hadamard product, and $\boldsymbol{M} \in \mathbb{B}^{U \times I}$ is a *mask matrix* having $\boldsymbol{M}_{u,i} = 1, \forall (u,i) \in \mathcal{K}$.

A.6 Main Results

Below, we summarized the results used in the paper; see Authors (Oct 2017) for the proofs.

We use following known result to find the descent direction for the FW method (the proof is known).

Proposition 2 *Consider the following Linear Program (LP),*

$$(P_{PS}) \ \ \boldsymbol{x}^\star = \operatorname*{argmin}_{\boldsymbol{x} \in \mathbb{R}^n} \boldsymbol{c}^T \boldsymbol{x}, \ \ \text{s. t.} \ \ \mathbf{1}^T \boldsymbol{x} = 1, \ \boldsymbol{x} \geq \mathbf{0}$$

Its optimal solution is given by

$$\boldsymbol{x}^\star = \boldsymbol{e}_{j^\star}\ \text{, where}\ \ j^\star = \ \text{argmin}_{1\leq j\leq n}\ \boldsymbol{c}^T\boldsymbol{e}_j$$

Thus, the solution reduces to searching over the vector $\boldsymbol{c}$. □

We show the convergence of the FW algorithm (Table 1).

Proposition 3 *Let* $\boldsymbol{\theta}_u^\star$ *be the optimal solution to* (Q_1)*. Then the sequence of iterates* $\{\boldsymbol{\theta}_u^{(k)}\}$ *satisfies (Jaggi, 2013)[Theorem 1],*

$$\|f(\boldsymbol{\theta}_u^{(k+1)}) - f(\boldsymbol{\theta}_u^\star)\|_2 \leq \mathcal{O}(1/k),\ k = 1, 2, \cdots \square$$

Proof: The linear convergence rate for all FW variants, was proved in Jaggi (2013)[Theorem 1].

Quasi-optimality of SDR: The question was studied extensively in the context of binary detection for multi-antenna communication (Tan & Rasmussen, 2001). Interestingly, (Q_2) can be recast as a noiseless binary detection problem, where SDR has been to be optimal. The results is formalized below.

Proposition 4 *Let* $g(\boldsymbol{\psi}_i^\star)$ *and* $g(\hat{\boldsymbol{\psi}}_i)$ *denote the optimal solutions to the binary QP in* (Q_2)*, and its SDR after randomization (Table 2), respectively. The approximation quality is defined as (Luo et al., 2010),*

$$\eta \leq\ g(\boldsymbol{\psi}_i^\star)/g(\hat{\boldsymbol{\psi}}_i)\ \leq 1. \tag{A.5}$$

It holds that $\eta = 1$*, with probability* $1 - \exp^{-\mathcal{O}(D)}$*, asymptotically in* D*. Thus, the relaxation is quasi-optimal.* □

Proof: See (Authors, Oct 2017).

Lemma 2 *Let* $t_n \triangleq \mathcal{E}(\{\boldsymbol{\psi}_i^{(n)}\}, \{\boldsymbol{\theta}_u^{(n)}\}),\ n = 1, 2, ...$ *be the sequence of iterates, resulting from the updates in Algorithm 1. Then,* $\{t_n\}$ *is non-increasing in* n*, and converges to a stationary point of* (Q) *in* (2)*, almost surely.* □

Proof: The convergence is shown in (Authors, Oct 2017).

A.7 Additional Numerical Results

Prediction Performance (Setting 2): Since the range of the predicted variable is different for MF/NMF/SVD++, and KM/NNM, we use the normalized test RMSE, i.e., NRMSE $= \eta(\sum_{(u,i)\in\bar{\mathcal{K}}} |[\boldsymbol{R}]_{(u,i)} - \hat{R}_{u,i}|^2/|\bar{\mathcal{K}}|)^{1/2}$ where $\bar{\mathcal{K}}$ is the test set, and $\eta = (R_{\max} - R_{\min})^{-1} = 1/4$ is the normalization for MF/NMF/SVD++. For KMs/NNMs the same metric reduces to NRMSE $= \left(\sum_{(u,i)\in\bar{\mathcal{K}}} |[\boldsymbol{R}]_{(u,i)}/R_{\max} - \hat{\boldsymbol{\theta}}_u^T\hat{\boldsymbol{\psi}}_i|^2/|\bar{\mathcal{K}}|\right)^{1/2}$. The best values for λ_u and μ_i, were picked from a coarse two-dimensional grid by cross-validation, using a held-out validation set. The Normalized RMSE results are shown in Table 4. We observe a significant gap between KMs, and well known collaborative filtering methods, especially as D increases. Moreover, the drop in performance for NNMs for increasing D may be due to over-fitting.

Asymptotic optimality of SDR for ψ-step solution: Table 5 is a numerical validation of Proposition 4 where we computed the error rate of SDR (compared to the exhaustive search), aggregated over all iterations. We observe that the approximation error decreases, with increasing D (following Proposition 4).

Table 4: Normalized Test RMSE (Setting 2). The dimension of factorization for MF/SVD++, k, is equal to D (unless stated in the corresponding entry). The normalized test RMSE for all other methods are taken from the following repository: `http://www.mymedialite.net/examples/datasets.html` ('-' indicates the unavailability of the correspond test RMSE from the repository.

	$D = 4$	$D = 8$	$D = 16$	$D = 24$
KM	0.199	**0.2013**	**0.1900**	**0.1861**
NNM	**0.194**	0.2255	0.2057	0.2118
MF	0.229	$0.228(k = 10)$	$-$	$0.226(k = 40)$
SVD++	0.228	$0.227(k = 10)$	$0.227(k = 20)$	$0.226(k = 50)$
K-M	0.210	.2096	0.2105	0.2105
NMF	$-$	$-$	$-$	$0.192(k = 100)$

Table 5: Error rate for SDR (Artificial Dataset, $U = 20, I = 40$).

	$D = 4$	$D = 8$	$D = 10$
SDR Accuracy $\times 10^{-3}$	7.5	4.4	4.0